ChemPubSoc Europe

DOI: 10.1002/ejic.201600163

EurJIC European Journal of Inorganic Chemistry

Full Paper

Tetradentate Ligands

Coordination Chemistry of an Unsymmetrical Naphthyridine-Based Tetradentate Ligand toward Various Transition-Metal Ions

Bing-Chen Tsai,[a] Yi-Hung Liu,[a] Shie-Ming Peng,[a] and Shiuh-Tzung Liu*[a]

Abstract: An unsymmetrical ligand, 2-(2-pyridinyl)-7-(pyrazol-1-yl)-1,8-naphthyridine ($\mathbf{L_5}$) was prepared for the construction of a series of dinuclear complexes. Treatment of $\mathbf{L_5}$ with $[Ru_2(\mu\text{-}OAc)_4Cl]$ followed by anion metathesis afforded $[(\mathbf{L_5})(\mu\text{-}OAc)_3Ru_2](PF_6)$ (**3**). Reaction of $\mathbf{L_5}$ with 2 equiv. of $Ni(OAc)_2$ provided $[Ni_4(\mathbf{L_5})_2(\mu\text{-}OH)_4(CF_3COO)_2](CF_3COO)_2$ (**5**). Reaction of $[Re_2(CO)_8(CH_3CN)_2]$ with $\mathbf{L_5}$ in a refluxing chlorobenzene solution gave a mixture of dirhenium (**6**) and monorhenium (**7**) complexes. The monocobalt complex **8** was obtained from complexation of $\mathbf{L_5}$ with $CoCl_2$. These new complexes were characterized by elemental analysis and spectroscopic techniques. The structures of complexes **3**, **5** and **8** were further confirmed by X-ray crystallography. Nickel complex **5** was evaluated as a catalyst for reduction reactions involving the conversion of ester functionalities into their corresponding alcohols.

Introduction

Whereas dinuclear metal complexes have, for several years, been an attractive topic in coordination chemistry and catalysis circles, the number of recent investigations into these species have increased dramatically.[1] Compared to monometallic species, dimetallic complexes can exhibit possible synergistic effects by virtue of interactions between the metal centers; such effects might lead to improvements in reactivity and/or selectivity.[1] In order to have an efficient interaction between metal ions for catalysis, Feringa et al. proposed that the optimum distance between the two metal centers is between 3.5 and 6.0 Å.[1d] Accordingly, the introduction of ligands able to accommodate metal ions in close proximity to each other has received much attention. Among various ligands designed for dinuclear systems, 2,7-disubstituted 1,8-naphthyridine-based ligands ($\mathbf{L_1}$–$\mathbf{L_4}$) (Figure 1) have been extensively employed in the construction of dimetallic complexes containing two metal ions within a short distance.[2–16] Indeed, ligand $\mathbf{L_1}$ has been shown to form stable dirhodium [Rh–Rh 2.405(2) Å],[13] diruthenium [Ru–Ru 2.273(4) Å][4] and dicopper [Cu–Cu 3.094 Å] complexes.[13c,16j] In addition, the metal ions are separated by 3.22 Å in the dinickel complex based on ligand $\mathbf{L_2}$,[16i] 2.9534(2) Å in the dicopper complex based on ligand $\mathbf{L_3}$, and 2.449(1)–2.7328(5) Å in the dicopper complexes based on ligand $\mathbf{L_4}$.[15] As a continuation of our efforts to develop new dimetallic complexes, we report here the preparation of unsymmetrical naphthyridine-based ligand $\mathbf{L_5}$ (Figure 1) and its complexation with various metal ions.

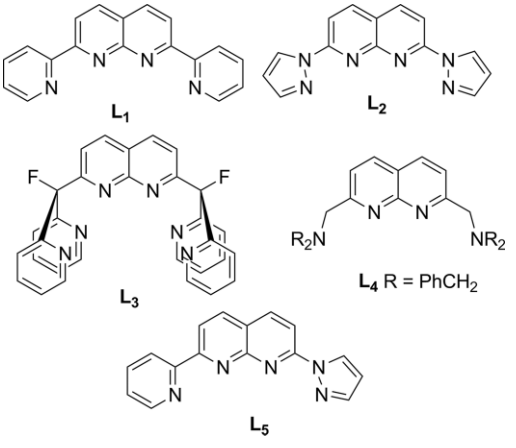

Figure 1. Selected 2,7-disubstituted naphthyridine-based ligands.

The reduction of esters to their corresponding alcohols is a practical approach to generating desired starting materials in organic synthesis. The reduction of ester functionalities using sodium borohydride is relatively difficult due to the low reactivity of the reducing agent.[17] However, the reducing power of $NaBH_4$ can be enhanced with the assistance of transition metal complexes. Among various metal salts, nickel complexes are known to be good catalysts in this regard.[18] In this work, we also report the effective reduction of esters using a newly prepared dinickel complex as a catalyst, and we endeavor to understand possible synergistic effects unique to the dimetallic system in question.

Results and Discussion

Preparation and Characterization of $\mathbf{L_5}$

The desired ligand, 2-(2-pyridinyl)-7-(pyrazol-1-yl)-1,8-naphthyridine ($\mathbf{L_5}$), was prepared by double substitution reactions of 2,7-

[a] Department of Chemistry, National Taiwan University,
1, Sec. 4, Roosevelt Road, Taipei 10617, Taiwan
E-mail: stliu@ntu.edu.tw
http://www.ch.ntu.edu.tw/
ORCID(s) from the author(s) for this article is/are available on the WWW under http://dx.doi.org/10.1002/ejic.201600163.

dichloro-1,8-naphthyridine (**1**) (Scheme 1). First, the introduction of the pyridinyl group was achieved by a Stille coupling reaction of **1** with 2-(tributylstannyl)pyridine to give **2** in 34 % isolated yield. Subsequently, thermal reaction of **2** with excess pyrazole rendered $\mathbf{L_5}$ in 75 % yield. Ligand $\mathbf{L_5}$ was characterized by NMR spectroscopy and mass spectrometry. ESI-HR mass spectra of $\mathbf{L_5}$ showed a peak at m/z = 274.1093, which is consistent with the molecular formula $C_{16}H_{11}N_5$ + 1 [M + H]. Figure 2 shows the ^{1}H NMR spectra of $\mathbf{L_1}$, $\mathbf{L_2}$ and $\mathbf{L_5}$ for the purposes of comparison. The ^{1}H NMR signals for H-6, H-7, and H-8 appear in the range of δ = 8.29–8.35 ppm as a complicated multiplet, showing the unsymmetrical nature of the molecule. The signals representative of H-10 and H-11 appear at δ = 6.53 and 8.97 ppm, respectively, which are similar to those observed for $\mathbf{L_2}$ (δ = 6.65 and 8.86 ppm).

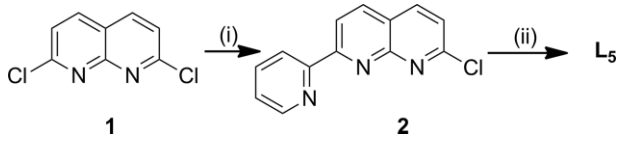

Scheme 1. Synthesis of $\mathbf{L_5}$. (i) (2-pyridinyl)$SnBu_3$, $PdCl_2(PPh_3)_2$, toluene, reflux; (ii) pyrazole, 110 °C.

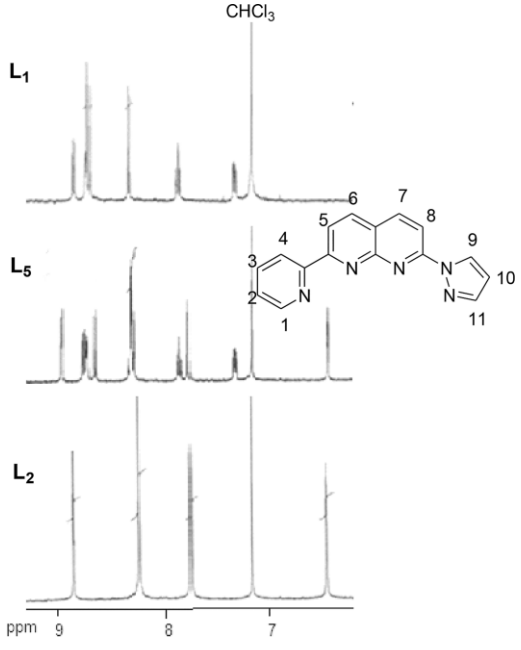

Figure 2. Comparison of the ^{1}H NMR spectra of $\mathbf{L_1}$, $\mathbf{L_2}$ and $\mathbf{L_5}$.

Diruthenium Complex 3

Dark purple complex **3** was prepared by reaction of $[Ru_2(\mu\text{-}OAc)_4Cl]$ with $\mathbf{L_5}$ in methanol followed by anion exchange (Scheme 2). Complex **3** is air-stable both in the solid state and in solution. It is slightly soluble in organic solvents such as $CHCl_3$, CH_2Cl_2 and diethyl ether, and much more soluble in acetone and acetonitrile. ESI-MS analysis of **3** revealed a peak at m/z = 653.9510 for the ion $[Ru_2(\mathbf{L_5})(\mu\text{-}OAc)_3]^+$, consistent with the formula of the cationic portion of **3**. The molecular configuration of **3** was unequivocally confirmed by X-ray crystallographic analysis. The ORTEP plot of **3** is shown in Figure 3, and some selected bond lengths and angles of **3** and $[Ru_2(\mathbf{L_1})(\mu\text{-}OAc)_3](PF_6)$ (**4**),[14] for comparison, are summarized in Table 1.

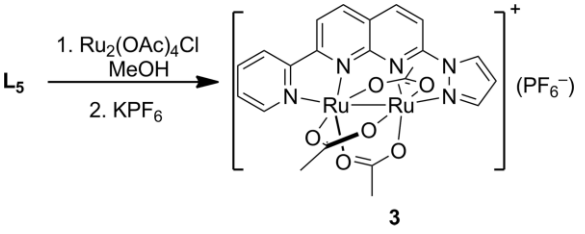

Scheme 2. Preparation of diruthenium complex **3**.

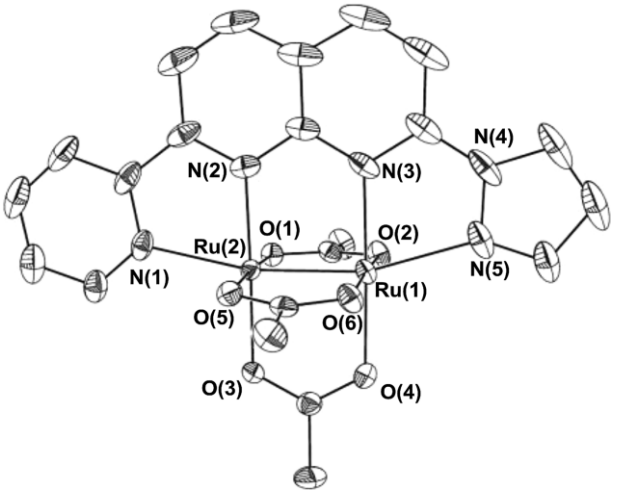

Figure 3. ORTEP plot of complex **3** (30 % probability level).

Table 1. Selected bond length and bond angles.

	Complex **3**	$[(\mathbf{L_1})Ru_2(\mu\text{-}OAc)_3]$ (**4**)[a]
Ru(1)–Ru(2)	2.2764(4)	2.28(2)
Ru(1)–N(5)	2.300(4)	2.24(2)
Ru(1)–N(3)	2.061(3)	2.05(2)
Ru(2)–N(2)	2.029(3)	2.00(2)
Ru(2)–N(1)	2.239(3)	2.21(2)
N(1)–Ru(2)–N(2)	76.71(15)	78.1(6)
N(1)–Ru(2)–Ru(1)	168.28(10)	167.2(4)
O(1)–Ru(2)–O(5)	176.28(10)	175.6(7)
N(2)–Ru(2)–O(3)	178.49(13)	178.7(6)
N(3)–Ru(1)–N(5)	74.41(15)	77.1(6)
N(5)–Ru(1)–Ru(2)	163.74(11)	167.7(5)
O(2)–Ru(1)–O(6)	175.86(11)	176.0(7)
N(3)–Ru(1)–O(4)	178.27(13)	179.8(9)

[a] Ref.[14]

The X-ray structure of **3** shows two ruthenium ions bridged by $\mathbf{L_5}$ and three acetate ligands resulting in what looks like a paddlewheel structure, which is similar to that of **4**, and is in line with expectations. The geometry around the ruthenium centers can be described as a distorted octahedron. The distance of Ru(1)–Ru(2) in **3** is 2.2763(4) Å, which is essentially identical to that found in **4**, indicative of typical metal–metal bonding. The 2-pyridinyl and 1-pyrazole groups occupy the axial sites *trans* to the Ru–Ru bond. The distance for the Ru(1)–

$N(5)_{pyrazolyl}$ linkage is slightly longer than that of the Ru(1)–N(5) bond. Other than this difference, all other bond lengths and angles in **3** are comparable with those observed in **4**.

Dinickel Complex 5

Under reflux conditions, reaction of $\mathbf{L_5}$ with 2 equiv. of $Ni(OAc)_2$ in methanol/CF_3COOH (3:1) provided dinickel complex **5** (Scheme 3). Complex **5** exists in a dimeric form as $[Ni_2(\mathbf{L_5})(CF_3COO)(\mu\text{-}OH)_2(H_2O)](CF_3COO)$ with the trifluoroacetate and hydroxy groups as the bridging ligands. ESI-MS analysis of **5** showed a peak at m/z = 727.9282 for the ion $[Ni_2(\mathbf{L_5})(CF_3COO)_3]^+$, indicative of the dinickel framework of the structure. The UV/Vis absorption spectrum of **5** in methanol exhibits bands at 357 and 372 nm ($\log \varepsilon$ = 4.19 and 4.25 M^{-1} cm^{-1}, respectively) attributable to charge transfer transitions. In addition, complex **5** shows a weak d–d transition at 659 nm, suggesting octahedral coordination around the Ni center.[19]

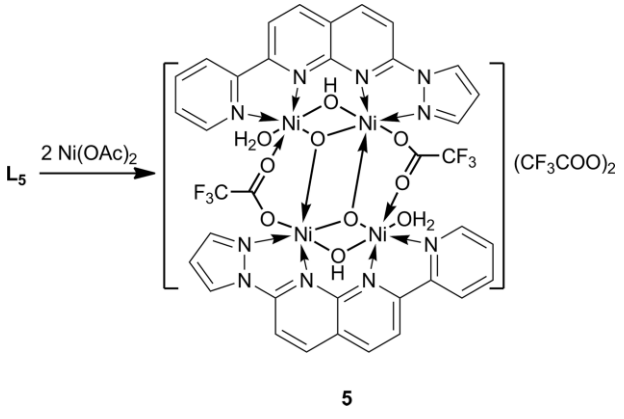

Scheme 3. Preparation of dinickel complex **5**.

The crystal structure of **5** contains a discrete $[Ni_4(\mathbf{L_5})_2(\mu\text{-}OH)_4(CF_3COO)_2(H_2O)_2]^{2+}$ cation and two trifluoroacetate anions. An ORTEP plot of the cationic portion of **5** is shown in Figure 4;

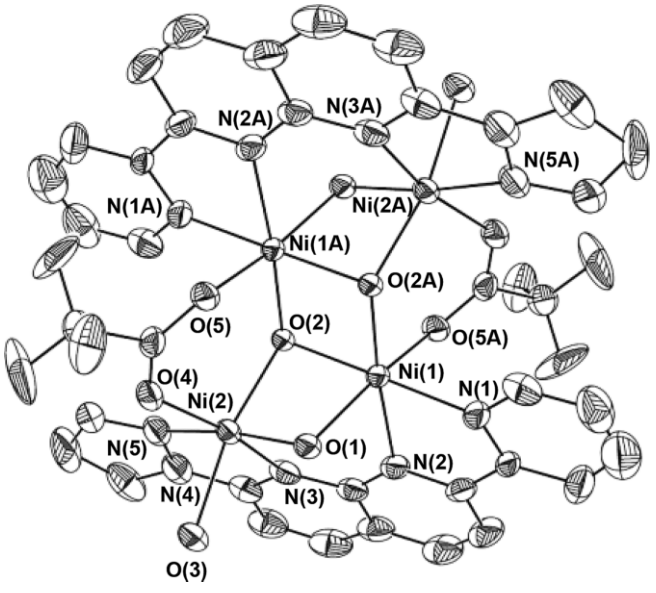

Figure 4. ORTEP plot of complex **5** (30 % probability level).

selected bond lengths and angles are listed in Table 2. The cation consists of two (μ-OH)(μ-CF_3COO)-bridged dimers of $[Ni_2(\mu\text{-}OH)_2(CF_3COO)]^+$. Each ligand $\mathbf{L_5}$ coordinates two structurally similar six-coordinate Ni^{II} centers bridged by two hydroxy ligands. The assignment of the formal μ-hydroxy bridges was based on the required charge balance for the chemical composition. Each of the metal centers achieves a distorted-octahedral configuration with the two nickel atoms separated by 2.992 Å. The bridging angles of Ni(1)–O(1)–Ni(2) and Ni(1)–O(2)–Ni(2) are 90.11(10)° and 95.18(10)°, respectively. The bond lengths for all Ni–O linkages are not equal, but remain in the normal range. The bite angle of N(2)–Ni(1)–N(1) is similar to that of the N(3)–Ni(2)–N(5) angle, indicating no significant effect of the nitrogen donors from pyridinyl or pyrazol-1-yl groups on this parameter.

Table 2. Selected bond lengths [Å] and bond angles [°].

Ni(1)–N(1)	2.049(3)	Ni(2)–N(3)	2.122(3)
Ni(1)–N(2)	2.131(3)	Ni(2)–N(5)	2.054(3)
Ni(1)–O(2A)	2.018(2)	$Ni(2)–O(3)_{(water)}$	2.069(3)
N(2)–Ni(1)–N(1)	77.5(1)	N(3)–Ni(2)–N(5)	77.3(1)
O(2)–Ni(1)–N(1)	179.2(1)	N(5)–Ni(2)–O(1)	173.3(1)
O(2A)–Ni(1)–N(2)	174.8(1)	O(4)–Ni(2)–N(3)	166.7(1)
Ni(1)–O(1)–Ni(2)	90.1(1)	Ni(1)–O(2)–Ni(2)	95.2(1)

Dirhenium Complex 6

Reaction of $[Re_2(CO)_8(CH_3CN)_2]$ with an equimolar amount of $\mathbf{L_5}$ in a sealed tube with chlorobenzene as the solvent provided a mixture of air-stable di- and monorhenium complexes **6** and **7** in 61 % and 39 % isolated yields, respectively (based on ligand) (Scheme 4). Both complexes **6** and **7** were isolated by chromatography. Conversion of mononuclear species **7** into **6** can be achieved by reaction of **7** with $Re_2(CO)_{10}$. This observation is similar to those made during thermal reactions of $\mathbf{L_1}$ with carbonylrhenium compounds presented in our previous works.[16g]

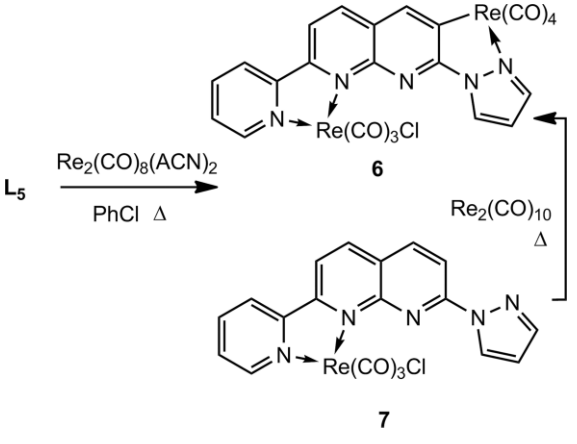

Scheme 4. Preparation of the rhenium complexes.

Both complexes **6** and **7** were characterized by spectroscopic methods. Carbonyl absorptions at 2013 cm^{-1} (sharp) and 1887 cm^{-1} (broad) in the IR spectrum of **7** are consistent with the existence of an $Re(CO)_3$ fragment, which is similar to the analogue $[(\mathbf{L_1})Re(CO)_3Cl]$. Coordination of a putative $Re(CO)_3Br$

fragment to the pyridinyl moiety in ligand $\mathbf{L_5}$, and not the pyrazolyl, is confirmed by ^{1}H NMR spectroscopic analysis. Both ^{1}H NMR spectra of $\mathbf{L_5}$ and **7** are shown in Figure 5 for the purposes of comparison. The signal for the C-1 proton shifts downfield significantly in complex **7**; this is not the case for the C-11 proton, clearly illustrating the coordination mode of the "bipyridine" moiety to the metal center. For complex **6**, the disappearance of the C-8 proton resonance in the ^{1}H NMR spectrum of **6** (Figure 6) suggests that metalation occurs at this position to yield the dinuclear species. The ESI-HR mass spectrum of **6** in an acetonitrile matrix shows a peak at m/z = 880.9976, consistent with the formula $[M - Cl + CH_3CN]^+$ (calcd. for $C_{25}H_{13}N_6O_7Re_2$ 880.9961). These observations clearly illustrate the structures of both complexes.

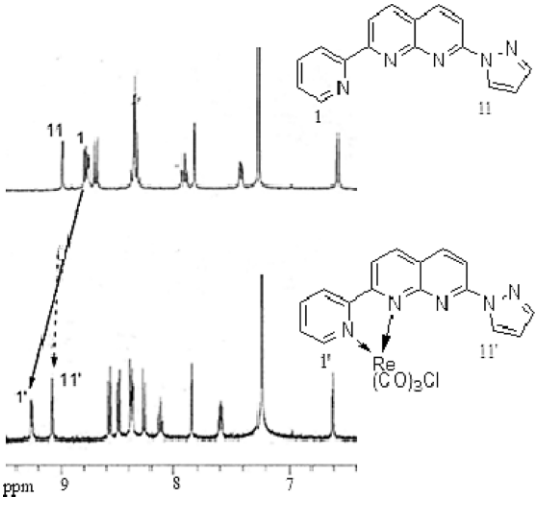

Figure 5. Comparison of the ^{1}H NMR spectra for $\mathbf{L_5}$ and **7**.

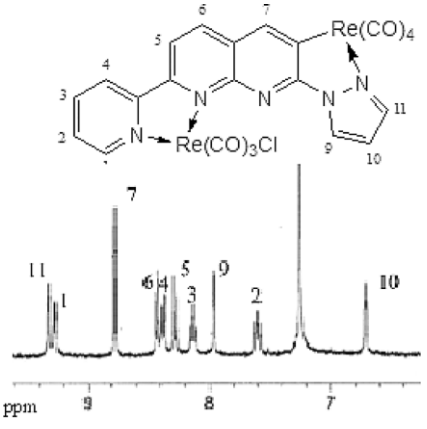

Figure 6. ^{1}H NMR spectrum of **6**.

Cobalt Complex 8

Reaction of $\mathbf{L_5}$ with 2 equiv. of $CoCl_2$ in anhydrous methanol under reflux conditions gave cobalt complex **8** as a bright green solid. ESI-HRMS analysis of the complex revealed two major peaks at m/z = 367.0056 and 768.9769, corresponding to the formulas of $[\mathbf{L_5} + CoCl]^+$ and $[\mathbf{8} - Cl]^+$, respectively. However, the detailed structural features of **8** were confirmed by means of X-ray crystallography. The coordination motif for complex **8** is depicted in Figure 7. The complex is a bis(chloride)-bridged Co^{II} dimer in which two metal ions are related to each other through an inversion center which bisects Co(1) and Co(1A) and also Cl(1) and Cl(1A). The geometry of each cobalt ion is described as a distorted trigonal-bipyramidal structure, and the coordination environment comprises two nitrogen donors from $\mathbf{L_5}$, two terminal chloride ions, and a bridging chloride ion. The axial sites are occupied by the naphthyridine nitrogen atoms [N(2)] and the bridging chloride ion [Cl(1A)]. Thus, the distance for the Co(1)–N(2) linkage [2.133(5) Å] is slightly longer than that of the Co(1)–N(1) bond [2.097(5) Å].

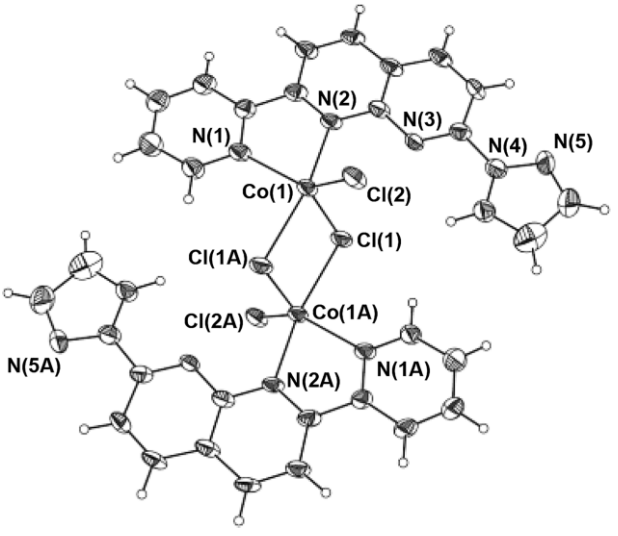

Figure 7. ORTEP plot of cobalt complex **8** (30 % probability level). Selected bond lengths [Å] and angles[°]: Co(1)–N(1) 2.097(5), Co(1)–N(2) 2.133(5), Co(1)–Cl(1) 2.339(2), Co(1)–Cl(2) 2.290(2); N(1)–Co(1)–N(2) 76.6(2), N(1)–Co(1)–Cl(2) 126.9(2), N(1)–Co(1)–Cl(1) 116.1(1), Cl(2)–Co(1)–Cl(1) 116.86(7).

Reduction of Esters Catalyzed by Dinickel Complex 5

Among these newly prepared complexes, we investigated the ability of dinickel complex **5** to catalyze the reduction of esters to their corresponding alcohols; such reductions constitute a useful approach to desired precursors in organic synthesis.

In this study, the reduction of methyl benzoate to benzyl alcohol was chosen as the model reaction to establish optimal catalytic conditions. In a typical experiment, a mixture of $PhCO_2Me$, $NaBH_4$ and nickel complex was heated to a specific temperature in either THF or diethyl ether. Crude products were analyzed by ^{1}H NMR spectroscopy, and results are summarized in Table 3. The reduction proceeded smoothly to provide the benzyl alcohol when using **5** as the catalyst. By screening various parameters it was ultimately determined that ideal conditions involved the use of $ZnCl_2$ as an additive with THF as the solvent at a reaction temperature of 45 °C (Table 3, Entry 6). Presumably, $ZnCl_2$ plays some role in the reduction by virtue of its Lewis acid character.[20] Evaluation of various nickel complexes as catalysts for this reduction revealed the clear overall superiority of complex **5** (Table 3, Entries 10–14).

Table 3. Reduction of PhCOOMe catalysed by **5** and related Ni complexes.[a]

Entry	Cat. (mol-%)	Additive	Solvent	Temp [°C]	Yield [%][b]
1	**5** (1.5)	–	THF	r.t.	10
2	**5** (1.5)	–	THF	65	54
3	**5** (1.5)	$ZnCl_2$	THF	65	92
4	**5** (1.5)	$ZnBr_2$	THF	65	90
5	**5** (1.5)	LiCl	THF	65	85
6	**5** (1.5)	$ZnCl_2$	THF	45	95
7	**5** (0.75)	$ZnCl_2$	THF	45	59
8	**5** (1.5)	$ZnCl_2$	Et_2O	40	52
9	**5** (1.5)	$ZnCl_2$	EtOH	65	17
10	$NiCl_2$ (3)	$ZnCl_2$	THF	45	38
11	**9** (1.5)[c]	$ZnCl_2$	THF	45	83
12	**10** (3)[c]	$ZnCl_2$	THF	45	48
13	**11** (3)[c]	$ZnCl_2$	THF	45	52
14	**10** + **11** (1.5 each)	$ZnCl_2$	THF	45	53

[a] Reaction conditions: A mixture of methyl benzoate (0.3 mmol), additive (0.3 mmol), Ni complex and $NaBH_4$ (0.6 mmol) in solvent (1 mL) was stirred for 12 h. [b] NMR-based yields. [c] Complexes **9**–**11** are shown in Scheme 5.

All the nickel complexes tested appear to exert catalytic activities in this reduction, although significant differences were noted. Both complexes **5** and **9** (Scheme 5) are dinuclear systems, and showed higher efficiency relative to their mononuclear analogues. This observation suggests that some cooperative effect between adjacent metal centers within the dimetallic systems, which is absent in mononuclear systems, may benefit such reductions.

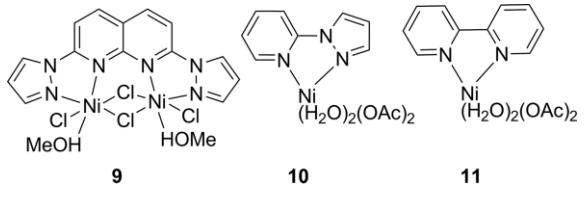

9 **10** **11**

Scheme 5. Nickel complexes as catalysts for the reduction of PhCOOMe.

According to proposals by Jones and James,[21] the cooperativity index (α) for a dimetallic system is formulated as $\alpha = (A_o - A_p)/A_{ave}$, where A_o is the observed activity of the dimetallic complex, A_p is the predicted activity of the dimetallic complex, $A_P = A_1 + A_2$ where A_1 is the measured activity of the monometallic complex that closely mimics the first center and A_2 is the measured activity of the second center, and finally, $A_{ave} = (A_1 + A_2)/2$. Taking the performance of the mixture of **10** and **11** (Scheme 5) as A_p, the cooperativity index (α) of **5** in this catalysis is 1.53, which is slightly larger than unity. This result does, in fact, suggest that **5** benefits from a slight cooperativity effect during the course of benzoate reduction.

With optimized reaction conditions now in hand, we explored the generality of this catalysis with other esters including lactones (Table 4). All benzoates with various substituents were found to undergo reduction to afford the respective benzyl alcohols in good to excellent yields (Table 4, Entries 1–7). This catalytic system also readily effected reduction of various lactones leading to production of the corresponding diols (Table 4, Entries 9–13). It was also noticed that α,β-unsaturated esters were fully reduced to the related alkyl alcohols (Table 4, Entries 14–16). Despite this apparently high level of activity, these dimetallic reducing conditions failed to reduce the amide functional group (Table 4, Entry 18).

Table 4. Reduction of esters as catalysed by complex **5**.[a]

Entry	Substrate	Product	Yield[b]
1	C_6H_5COOPh	$C_6H_5CH_2OH$	90%
2	C_6H_5COOEt	$C_6H_5CH_2OH$	89%
3	*p*-$MeOC_6H_4COOEt$	*p*-$MeOC_6H_4CH_2OH$	88%
4	*p*-ClC_6H_4COOEt	*p*-$ClC_6H_4CH_2OH$	92%
5	*p*-BrC_6H_4COOEt	*p*-$BrC_6H_4CH_2OH$	91%
6	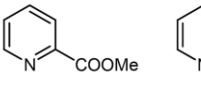	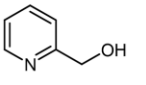	89%
7	*o*-$C_6H_4(COOMe)_2$	*o*-$C_6H_4(CH_2OH)_2$	75%
8	$C_6H_5CH_2COOMe$	$C_6H_5CH_2CH_2OH$	90%
9	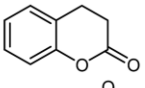	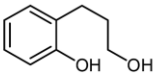	74%
10	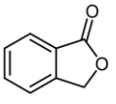	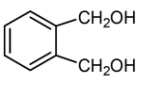	85%
11	4-butanolide	$HO(CH_2)_4OH$	81%
12	5-pentanolide	$HO(CH_2)_5OH$	79%
13	6-hexanolide	$HO(CH_2)_6OH$	76%
14	$C_6H_5CH{=}CHCO_2Ph$	$C_6H_5(CH_2)_3OH$	95%
15	$CH_3CH{=}CHCOOMe$	$CH_3CH_2CH_2OH$	89%
16	dimethyl maleate	$HO(CH_2)_4OH$	87%
17	succinic anhydride	$HO(CH_2)_4OH$	78%
18	$C_6H_5CONHPh$	–	–

[a] Reaction conditions: A mixture of ester (0.3 mmol), $ZnCl_2$ (0.3 mmol), **5** (4.5×10^{-3} mmol) and $NaBH_4$ (0.6 mmol) in THF (1 mL) was stirred at 45 °C for 12 h. [b] Isolated yields.

Conclusions

We have prepared a set of dinuclear complexes based on an unsymmetric ligand, 2-(2-pyridinyl)-7-(pyrazol-1-yl)-1,8-naphthyridine (**L_5**). Both ruthenium and nickel complexes are dinuclear systems with short metal–metal distances, Ru–Ru (2.2763 Å) in **3** and Ni–Ni (2.992 Å) in **5**. The distance between nickel atoms in **5** is significantly shorter than that found in **9**. For **6**, two metal ions are not seated in the "pocket" of **L_5**. Rather, in this case, one of the metal centers underwent *o*-metallation at the naphthyridine ring. From the observed formation of complexes **7** and **8**, we established that the chelation ability of the bipyridine moiety in **L_5** is superior to that of the pyridine–pyrazole moiety. In addition, nickel species **5** is an effective catalyst for the reduction of esters and lactones. Other transition metal complexes containing **L_5** were also prepared, but their precise structures not yet elucidated. Studies of the coordination chemistry of **5** with other metal ions are currently underway.

Experimental Section

General: Chemicals and solvents were of analytical grade and used without further purification. NMR spectra were recorded with a 400 MHz spectrometer. Chemical shifts are given in ppm relative to Me_4Si for ^1H and ^{13}C NMR spectra. Compound **1** was prepared according to a previously reported method.[16b]

2-Chloro-7-(pyridin-2-yl)-1,8-naphthyridine (2): A mixture of 2,7-dichloro-1,8-naphthyridine (**1**) (1.0 g, 5.0 mmol), 2-(tributylstannyl)pyridine (2.8 g, 7.5 mmol) and $PdCl_2(PPh_3)_2$ (178 mg, 0.25 mmol) in pre-dried toluene (60 mL) was heated at reflux temperature under an inert gas for 48 h. After removal of the toluene, the residue was washed with hexane to remove the unreacted 2-(tributylstannyl)pyridine. The residue was chromatographed on silica gel with elution of dichloromethane/ethyl acetate (5:1, v/v) to give **1** as a yellow solid (400 mg, 34 %). ^1H NMR (400 MHz, $CDCl_3$): δ = 8.81 (d, J = 8 Hz, 1 H), 8.74 (d, J = 8 Hz, 1 H), 8.7–8.72 (m, 1 H), 8.29 (d, J = 8 Hz, 1 H), 8.14 (d, J = 8 Hz, 1 H), 7.86 (t, J = 8 Hz, 1 H), 7.48 (d, J = 8 Hz, 1 H), 7.36–7.39 (m, 1 H) ppm. This compound was used for the next step of synthesis without further characterization.

2-(Pyrazol-1-yl)-7-(pyridin-2-yl)-1,8-naphthyridine (L_5): A mixture of **1** (48.1 mg, 0.2 mmol) and pyrazole (40.5 mg, 0.6 mmol) was heated in a sealed tube at 110 °C for 24 h. The resulting mixture was washed with water to remove excess pyrazole, and the residue was passed through a filtration column to give **L_5** as a light yellow solid (41.6 mg, 75 %). ^1H NMR (400 MHz, $CDCl_3$): δ = 8.97 (d, J = 2.6 Hz, 1 H), 8.77 (d, J = 8 Hz, 1 H), 8.72 (d, J = 8 Hz, 1 H), 8.66 (d, J = 8 Hz, 1 H), 8.29–8.35 (m, 3 H), 7.88 (t, J = 8 Hz, 1 H), 7.8 (d, J = 0.96 Hz, 1 H), 7.34–7.39 (m, 1 H), 6.53–6.54 (m, 1 H) ppm. ^{13}C NMR (100 MHz, $CDCl_3$): δ = 159.8, 155.0, 154.3, 152.9, 149.0, 142.8, 139.4, 137.5, 136.8, 128.0, 124.5, 122.5, 121.4, 119.3, 113.4, 108.6 ppm. ESI-HRMS: calcd. for $C_{16}H_{12}N_5$ $[M + H]^+$ 274.1093, found 274.1092.

Diruthenium Complex 3: A mixture of **L_5** (24.6 mg, 0.09 mmol) and $Ru_2(OAc)_4Cl$ (48.3 mg, 0.10 mmol) in methanol (3 mL) was stirred at room temperature for 20 h. KPF_6 (18.8 mg, 0.10 mmol) was added to the mixture with stirring for another 2 h. After removal of the solvent, the mixture was dissolved in dichloromethane (10 mL) and washed with water (2 × 3 mL). The organic portion was dried and concentrated. Upon crystallization in methanol/diethyl ether, the desired compound was obtained as a purple solid (45.8 mg, 63 %). ESI-HRMS: calcd. for $C_{22}H_{20}N_5O_6Ru_2$ $[M - PF_6]^+$ 653.9501, found 653.9515. $C_{22}H_{20}F_6N_5O_6PRu_2$ (797.53): calcd. C 33.13, H 2.53, N 8.78; found C 33.06, H 2.07, N 8.59.

Dinickel Complex 5: A mixture of **L_5** (28 mg, 0.10 mmol) and $Ni(OAc)_2{\cdot}4H_2O$ (58 mg, 0.23 mmol) in a mixed solvent MeOH (3 mL)/CF_3COOH (1 mL) was heated in an oil bath at 100 °C for 18 h. Upon cooling, slow addition of diethyl ether to the reaction mixture gave a green precipitate (43 mg, 64 %) as the desired complex. UV/Vis (MeOH): λ_{max} (log ε) = 659 (0.39), 372 (4.25), 357 (3.19), 262 (4.27), 249 (4.25), 212 (4.18 M^{-1} cm^{-1}) nm. Conductivity (MeOH): 89.1 Ω^{-1} cm mol^{-1}. $C_{42}H_{31}F_{15}N_{10}Ni_4O_{16}$ (M + CF_3COOH) (1565.53): calcd. C 34.75, H 2.15, N 9.65; found C 34.74, H 2.15, N 9.94.

Rhenium Complexes 6 and 7: A mixture of **L_5** (20 mg, 0.07 mmol) and $Re_2(CO)_8(CH_3CN)_2$ (50 mg, 0.07 mmol) in chlorobenzene (2 mL) was loaded in a sealed tube. The mixture was heated at 200 °C for 4 h. After the reaction, the chlorobenzene was removed under reduced pressure, and the residue was chromatographed on silica gel by elution with ethyl acetate/acetone (5:1). Two bands on the column were separated and collected: red solid as complex **7** (16 mg, 39 %) and dark red solid as complex **6** (38 mg, 61 %). Complex **7**: IR (KBr): $\tilde{\nu}$ = 1887 (br.), 2013 cm^{-1}. ^1H NMR (400 MHz, $CDCl_3$): δ = 9.26 (d, J = 5.6 Hz, 1 H), 9.09 (d, J = 2.8 Hz, 1 H), 8.58 (d, J = 8.8 Hz, 1 H), 8.49 (d, J = 8.4 Hz,1 H), 8.38 (d, J = 8.8 Hz, 1 H), 8.37 (d, J = 8 Hz, 1 H), 8.26 (d, J = 8.4 Hz, 1 H), 8.12 (t, J = 8 Hz, 1 H), 7.85 (s, 1 H), 7.59 (t, J = 8 Hz, 1 H), 6.61 (dd, J = 2.8, 2 Hz,1 H) ppm. ESI-HRMS: calcd. for $C_{19}H_{11}ClN_5NaO_3Re$ $[M + Na]^+$ 602.0006, found 602.0008. $C_{19}H_{11}ClN_5O_3Re$ (578.98): calcd. C 39.41, H 1.91, N 12.10; found C 39.03, H 1.66, N 11.86. Complex **6**: IR (KBr): $\tilde{\nu}$ = 1899–2016 (br.), 2097 cm^{-1}. ^1H NMR (400 MHz, $CDCl_3$): δ = 9.32 (d, J = 2 Hz, 1 H), 9.27 (d, J = 4.8 Hz, 1 H), 8.78 (s, 1 H), 8.43 (d, J = 8.4 Hz, 1 H), 8.38 (d, J = 8.4 Hz, 1 H), 8.28 (d, J = 8.8 Hz,1 H), 8.13 (t, J = 8 Hz, 1 H), 7.97 (s, 1 H), 7.60 (t, J = 6 Hz, 1 H), 6.71 (s,1 H) ppm. ESI-HRMS: calcd. for $C_{25}H_{13}N_6O_7Re_2$ $[M - Cl + CH_3CN]^+$ 880.9933, found 882.9976. $C_{23}H_{10}ClN_5O_7Re_2$ (876.21): calcd. C 31.53, H 1.15, N 7.99; found C 31.33, H 1.24, N 7.63.

Cobalt Complex 8: A mixture of **L_5** (30 mg, 0.11 mmol) and $CoCl_2$ (29 mg, 0.23 mmol) in anhydrous methanol (2 mL) was heated at reflux under nitrogen for 24 h. After cooling, addition of diethyl ether to the reaction mixture gave complex **8** as a bright green solid (33 mg, 75 %). UV/Vis (MeOH): λ_{max} (log ε) = 416 (2.48), 371 (4.49), 356 (4.10), 260 (4.21), 249 (4.21), 212 (4.13 M^{-1} cm^{-1}) nm. ESI-HRMS: calcd. for $C_{16}H_{11}ClCoN_5$ [1/2M – Cl]$^+$ 367.0035, found 367.0055. $C_{32}H_{22}Cl_4Co_2N_{10}$ (806.27): calcd. C 47.67, H 2.75, N 17.37; found C 47.29, H 2.55, N 17.00.

Catalytic Reduction of Ester Substrates: A mixture of ester (0.3 mmol), $ZnCl_2$ (41 mg, 0.3 mmol), Ni complex **5** (6 mg, 4.5×10^{-3} mmol) and $NaBH_4$ (23 mg, 0.6 mmol) in THF (1 mL) was stirred at 45 °C for 12 h. After completion of the reaction, 1 M HCl (2 mL) was added and the mixture extracted with diethyl ether (2 × 5 mL). The organic extracts were combined and dried with $MgSO_4$. The desired product was purified by chromatography with hexane/EtOAc as eluent. All reduced products are known compounds, and their spectral analyses are in agreement with the reported data.

Benzyl Alcohol: Yield 29.3 mg, 90 %. ^1H NMR (400 MHz, $CDCl_3$): δ = 7.35–7.38 (m, 5 H), 4.59 (s, 2 H) ppm. ^{13}C NMR (100 MHz, $CDCl_3$): δ = 140.7, 128.2, 127.2, 126.8, 64.5 ppm.

4-Methoxybenzyl Alcohol: Yield 36.5 mg, 88 %. ^1H NMR (400 MHz, $CDCl_3$): δ = 7.24 (d, J = 8.4 Hz, 2 H), 6.86 (d, J = 8.4 Hz, 2 H), 4.53 (s, 2 H), 3.78 (s, 3 H), 2.63 (br., 1 H) ppm. ^{13}C NMR (100 MHz, $CDCl_3$): δ = 158.9, 133.0, 128.5, 113.7, 64.6, 55.1 ppm.

4-Chlorobenzyl Alcohol: Yield 39.4 mg, 92 %. ^{1}H NMR (400 MHz, $CDCl_3$): δ = 7.29 (d, J = 8.4 Hz, 2 H), 7.22 (d, J = 8.4 Hz, 2 H), 4.56 (s, 2 H), 2.82 (br., 1 H) ppm. ^{13}C NMR (100 MHz, $CDCl_3$): δ = 139.1, 133.2, 128.5, 128.3, 64.2 ppm.

4-Bromobenzyl Alcohol: Yield 51.2 mg, 91 %. ^{1}H NMR (400 MHz, $CDCl_3$): δ = 7.47 (d, J = 8.8 Hz, 2 H), 7.24 (d, J = 8.8 Hz, 2 H), 4.64 (s, 1 H) ppm. ^{13}C NMR (100 MHz, $CDCl_3$): δ = 139.7, 131.6, 128.6, 121.4, 64.5 ppm.

2-(Hydroxymethyl)pyridine: Yield 29.1 mg, 89 %. ^{1}H NMR (400 MHz, $CDCl_3$): δ = 8.51 (d, J = 4.8 Hz, 1 H), 7.64–7.68 (m, 1 H), 7.27 (d, J = 8 Hz, 1 H), 7.15–7.19 (m, 1 H), 4.74 (s, 1 H), 3.95 (br., 1 H) ppm. ^{13}C NMR (100 MHz, $CDCl_3$): δ = 159.3, 148.4, 136.7, 122.3, 120.6, 64.2 ppm.

Benzene-1,2-dimethanol: Yield 35.2 mg, 85 %. ^{1}H NMR (400 MHz, $CDCl_3$): δ = 7.26 (m, 4 H), 4.53 (s, 4 H), 4.42 (br., 2 H) ppm. ^{13}C NMR(100 MHz, $CDCl_3$): δ = 139.0, 129.3, 128.2, 63.3 ppm.

3-(*o*-Hydroxyphenyl)-1-propanol: Yield 35.9 mg, 74 %. ^{1}H NMR (400 MHz, $CDCl_3$): δ = 7.08–7.12 (m, 2 H), 6.84–6.90 (m, 2 H), 3.65 (t, J = 6.4 Hz, 2 H), 2.78 (t, J = 7.2 Hz, 2 H), 1.85–1.92 (m, 2 H) ppm. ^{13}C NMR (100 MHz, $CDCl_3$): δ = 154.1, 130.5, 127.5, 127.3, 120.6, 115.6, 60.9, 32.2, 25.4 ppm.

2-Phenylethanol: Yield 33.0 mg, 90 %. ^{1}H NMR (400 MHz, $CDCl_3$): δ = 7.30–7.34 (m, 2 H), 7.23–7.26 (m, 3 H), 3.84 (t, J = 6.4 Hz, 2 H), 2.86 (t, J = 6.4 Hz, 2 H), 1.88 (br., 1 H) ppm. ^{13}C NMR (100 MHz, $CDCl_3$): δ = 138.5, 129.0, 128.5, 126.4, 63.5, 39.1 ppm.

1,4-Butanediol: Yield 21.9 mg, 81 %. ^{1}H NMR (400 MHz, $CDCl_3$): δ = 3.63 (t, J = 6 Hz, 4 H), 3.08 (br., 1 H), 1.61–1.67 (m, 4 H) ppm. ^{13}C NMR(100 MHz, $CDCl_3$): δ = 62.5, 29.8 ppm.

1,5-Pentanediol: Yield 24.7 mg, 79 %. ^{1}H NMR (400 MHz, $CDCl_3$): δ = 3.61 (t, J = 6.4 Hz, 4 H) 2.22 (br., 1 H), 1.53–1.60 (m, 4 H), 1.42–1.44 (m, 2 H) ppm. ^{13}C NMR (100 MHz, $CDCl_3$): δ = 62.5, 32.2, 21.9 ppm.

1,6-Hexanediol: Yield 26.9 mg, 76 %. ^{1}H NMR (400 MHz, $CDCl_3$): δ = 3.61 (t, J = 6 Hz, 4 H), 1.94 (br., 2 H), 1.53–1.57 (m, 4 H), 1.34–1.38 (m, 4 H) ppm. ^{13}C NMR (100 MHz, $CDCl_3$): δ = 62.7, 32.5, 25.4 ppm.

Crystallography: Crystals suitable for X-ray determination were obtained for **3**, **5**·$(CF_3COOH)_2(CH_3CN)_2$ and **8** by recrystallization. Cell parameters were determined using a Siemens SMART CCD diffractometer. The structures were solved using the SHELXS-97 program[22] and refined using the SHELXL-97 program[23] by full-matrix least squares on the F^2 values. CCDC 1453770 (for **3**), 1453771 (for **5**), and 1453772 (for **8**) contain the supplementary crystallographic data for this paper. These data can be obtained free of charge from The Cambridge Crystallographic Data Centre.

Crystal Data for 3: $C_{24}H_{23}F_6N_6O_6PRu_2$, F_w = 838.59, monoclinic, $P2_1/c$, a = 12.7015(2) Å, b = 31.9155(5) Å, c = 8.19920(10) Å, β = 104.634(2)°, V = 3215.92(8) Å^3, Z = 4, $D_{calcd.}$ = 1.732 Mg/m^3, F(000) = 1656, crystal size: 0.25 × 0.15 × 0.10 mm, θ = 2.97–27.49°, 35142 reflections collected, 7266 reflections [R(int) = 0.0294], final R indices [$I > 2\sigma(I)$]: $R1$ = 0.0361, $wR2$ = 0.1174, for all data $R1$ = 0.0432, $wR2$ = 0.1220, goodness-of-fit on F^2 = 1.153.

Crystal Data for 5: $C_{24}H_{19}F_9N_6Ni_2O_9$, F_w = 823.87, triclinic, $P\bar{1}$, a = 10.4810(3) Å, b = 12.7454(3) Å, c = 13.0431(4) Å, α = 77.674(3)°, β = 66.605(3)°, γ = 81.187(2)°, V = 1557.70(7) Å^3, Z = 2, $D_{calcd.}$ = 1.757 Mg/m^3, F(000) = 828, crystal size: 0.25 × 0.20 × 0.10 mm, θ = 2.98–27.49°, 14362 reflections collected, 6911 reflections [R(int) = 0.0285], final R indices [$I > 2\sigma(I)$]: $R1$ = 0.0499, $wR2$ = 0.1422, for all data $R1$ = 0.0695, $wR2$ = 0.1629, goodness-of-fit on F^2 = 1.093.

Crystal Data for 8: $C_{32}H_{22}Cl_4Co_2N_{10}$, F_w = 806.26, monoclinic, $P2_1/n$, a = 9.5111(7) Å, b = 17.3587(8) Å, c = 10.4103(8) Å, β = 110.918(8)°, V = 1605.47(19) Å^3, Z = 2, $D_{calcd.}$ = 1.668 Mg/m^3, F(000) = 812, crystal size: 0.20 × 0.15 × 0.10 mm, θ = 3.28–24.99°, 5831 reflections collected, 2799 reflections [R(int) = 0.0445], final R indices [$I > 2\sigma(I)$]: $R1$ = 0.0633, $wR2$ = 0.1641, for all data $R1$ = 0.1023, $wR2$ = 0.1899, goodness-of-fit on F^2 = 1.026.

Acknowledgments

We thank the Ministry of Science and Technology, Taiwan, for financial support (NSC103-2113-M-002-002-MY3).

Keywords: Dimetallic complexes · Nickel · Ruthenium · Rhenium · Naphthyridine · Reduction

[1] Recent reviews: a) M. Boiocchi, L. Fabbrizzi, *Chem. Soc. Rev.* **2014**, *43*, 1835–1847; b) J.-P. Launay, *Coord. Chem. Rev.* **2013**, *257*, 1544–1554; c) Y. Sunatsuki, R. Kawamoto, K. Fujita, H. Maruyama, T. Suzuki, H. Ishida, M. Kojima, S. Iijima, N. Matsumoto, *Coord. Chem. Rev.* **2010**, *254*, 1871–1881; d) E. K. van den Beuken, B. L. Feringa, *Tetrahedron* **1998**, *54*, 12985–13011.

[2] a) M. Sarkar, H. Doucet, J. K. Bera, *Chem. Commun.* **2013**, *49*, 9764–9766; b) P. Daw, T. Ghatak, H. Doucet, J. K. Bera, *Organometallics* **2013**, *32*, 4306–4313; c) A. Sinha, M. Majumdar, M. Sarkar, T. Ghatak, J. K. Bera, *Organometallics* **2013**, *32*, 340–349; d) S. M. W. Rahaman, D. Das, N. Sadhukhan, A. Sinha, J. K. Bera, *Inorg. Chim. Acta* **2011**, *374*, 320–326; e) J. K. Bera, N. Sadhukhan, M. Majumdar, *Eur. J. Inorg. Chem.* **2009**, 4023–4038; f) S. K. Patra, J. K. Bera, *Organometallics* **2007**, *26*, 2598–2603; g) S. K. Patra, J. K. Bera, *Organometallics* **2006**, *25*, 6054–6060; h) J. K. Bera, E. J. Schelter, S. K. Patra, J. Bacsa, K. R. Dunbar, *Dalton Trans.* **2006**, 4011–4019; i) S. K. Patra, N. Sadhukhan, J. K. Bera, *Inorg. Chem.* **2006**, *45*, 4007–4015.

[3] G.-M. Lin, M. Sigrist, E.-C. Horng, C.-h. Chen, C.-Y. Yeh, G.-H. Lee, S.-M. Peng, *Z. Anorg. Allg. Chem.* **2015**, *641*, 2258–2265.

[4] a) W.-F. Fu, L.-F. Jia, W.-H. Mu, X. Gan, J.-B. Zhang, P.-H. Liu, Q.-Y. Cao, G.-J. Zhang, L. Quan, X.-J. Lv, Q.-Q. Xu, *Inorg. Chem.* **2010**, *49*, 4524–4533; b) Y. Chen, J.-S. Chen, X. Gan, W.-F. Fu, *Inorg. Chim. Acta* **2009**, *362*, 2492–2498.

[5] a) T. C. Davenport, T. D. Tilley, *Dalton Trans.* **2015**, *44*, 12244–12255; b) T. C. Davenport, T. D. Tilley, *Angew. Chem. Int. Ed.* **2011**, *50*, 12205–12208; *Angew. Chem.* **2011**, *123*, 12413–12416.

[6] a) H. Araki, K. Tsuge, Y. Sasaki, S. Ishizaka, N. Kitamura, *Inorg. Chem.* **2007**, *46*, 10032–10034.

[7] X.-J. Su, M. Gao, L. Jiao, R.-Z. Liao, P. E. M. Siegbahn, J.-P. Cheng, M.-T. Zhang, *Angew. Chem. Int. Ed.* **2015**, *54*, 4909–4914; *Angew. Chem.* **2015**, *127*, 4991–4996.

[8] L. A. Wilkinson, L. McNeill, P. A. Scattergood, N. J. Patmore, *Inorg. Chem.* **2013**, *52*, 9683–9691.

[9] J. D. Aguirre, D. A. Lutterman, A. M. Angeles-Boza, K. R. Dunbar, C. Turro, *Inorg. Chem.* **2007**, *46*, 7494–7502.

[10] T. Tanase, H. Takenaka, E. Goto, *J. Organomet. Chem.* **2007**, *692*, 175–183.

[11] M. Basato, A. Biffis, G. Martinati, C. Tubaro, C. Graiff, A. Tiripicchio, L. A. Aronica, A. M. Caporusso, *J. Organomet. Chem.* **2006**, *691*, 3464–3471.

[12] T. Suzuki, *Inorg. Chim. Acta* **2006**, *359*, 2431–2438.

[13] a) W. R. Tikkanen, E. Binamira-Soriaga, W. C. Kaska, P. C. Ford, *Inorg. Chem.* **1984**, *23*, 141–146; b) W. R. Tikkanen, E. Binamira-Soriaga, W. C. Kaska, P. C. Ford, *Inorg. Chem.* **1983**, *22*, 1147–1148; c) W. R. Tikkanen, C. Krueger, K. D. Bomben, W. L. Jolly, W. C. Kaska, P. C. Ford, *Inorg. Chem.* **1984**, *23*, 3633–3638.

[14] E. Binamira-Soriaga, N. L. Keder, W. C. Kaska, *Inorg. Chem.* **1990**, *29*, 3167–3171.

[15] C. He, S. J. Lippard, *Inorg. Chem.* **2000**, *39*, 5225–5231.

[16] a) C.-H. Lee, C.-L. Wu, S.-A. Hua, Y.-H. Liu, S.-M. Peng, S.-T. Liu, *Eur. J. Inorg. Chem.* **2015**, 1417–1423; b) W.-H. Tang, Y.-H. Liu, S.-M. Peng, S.-T. Liu, *J. Organomet. Chem.* **2015**, *775*, 94–100; c) C.-Y. Huang, K.-Y. Kuan, Y.-H. Liu, S.-M. Peng, S.-T. Liu, *Organometallics* **2014**, *33*, 2831–2836; d) B.-S. Liao,

Y.-H. Liu, S.-M. Peng, K. R. Reddy, S.-H. Liu, P.-T. Chou, S.-T. Liu, *Dalton Trans.* **2014**, *43*, 3557–3562; e) M.-U. Hung, B.-S. Liao, Y.-H. Liu, S.-M. Peng, S.-T. Liu, *Appl. Organomet. Chem.* **2014**, *28*, 661–665; f) T.-C. Su, Y.-H. Liu, S.-M. Peng, S.-T. Liu, *Eur. J. Inorg. Chem.* **2013**, 2362–2367; g) Y.-S. Lan, B.-S. Liao, Y.-H. Liu, S.-M. Peng, S.-T. Liu, *Eur. J. Org. Chem.* **2013**, 5160–5164; h) T.-P. Cheng, B.-S. Liao, Y.-H. Liu, S.-M. Peng, S.-T. Liu, *Dalton Trans.* **2012**, *41*, 3468–3473; i) B.-S. Liao, Y.-H. Liu, S.-M. Peng, S.-T. Liu, *Dalton Trans.* **2012**, *41*, 1158–1164; j) Y.-H. Chang, Z.-Y. Liu, Y.-H. Liu, S.-M. Peng, J.-T. Chen, S.-T. Liu, *Dalton Trans.* **2011**, *40*, 489–494.

[17] S. T. Lin, J. A. Roth, *J. Org. Chem.* **1979**, *44*, 309–310.

[18] J. M. Khurana, P. Sharma, *Bull. Chem. Soc. Jpn.* **2004**, *77*, 549–552.

[19] L. K. Das, A. Biswas, J. S. Kinyon, N. S. Dalal, H. Zhou, A. Ghosh, *Inorg. Chem.* **2013**, *52*, 11744–11757.

[20] T. Yamakawa, M. Masaki, H. Nohira, *Bull. Chem. Soc. Jpn.* **2004**, *77*, 549–552.

[21] N. D. Jones, B. R. James, *Adv. Synth. Catal.* **2002**, *344*, 1126–1134.

[22] For information regarding SHELXS-90, see: G. M. Sheldrick, *Acta Crystallogr., Sect. A: Found. Crystallogr.* **1990**, *46*, 467.

[23] G. M. Sheldrick, *SHELXL-97*, University of Göttingen, Göttingen, Germany, **1997**.

Received: February 18, 2016
Published Online: April 26, 2016

